ACADEMIA ROMÂNĂ
Revue Roumaine de Chimie
http://web.icf.ro/rrch/

Rev. Roum. Chim.,
2018, *63*(5-6), 459-466

Dedicated to Dr. Maria Zaharescu
on the occasion of her 80th anniversary

SYNTHESIS OF COBALT ALUMINATE NANOPARTICLES BY COMBUSTION METHODS USING CINNAMON BARK EXTRACT

Dana GINGAŞU,[a*] Ioana MÎNDRU,[a] Luminița PATRON,[a] Gabriela MARINESCU,[a] Adelina IANCULESCU,[b] Vasile-Adrian SURDU,[b] Simona ŞOMĂCESCU,[a] Silviu PREDA[a] and Ovidiu OPREA[b]

[a] "Ilie Murgulescu" Institute of Physical Chemistry, Roumanian Academy, 202 Splaiul Independentei, 060021 Bucharest, Roumania
[b] "Politehnica" University of Bucharest, Faculty of Applied Chemistry and Materials Science, 1 – 7 Polizu Street, 011061 Bucharest, Roumania

Received July 7, 2017

Cobal aluminate ($CoAl_2O_4$) nanoparticles were synthesized through classic combustion (CCM) and microwave combustion (MCM) methods using cinnamon bark extract. X-ray diffraction (XRD), scanning electron microscopy (SEM), transmission electron microscopy (TEM), X-ray photoelectron spectroscopy (XPS), infrared spectroscopy (IR) and ultraviolet–visible (UV–vis) spectroscopy were used for the characterization of the cobalt aluminate nanoparticles.

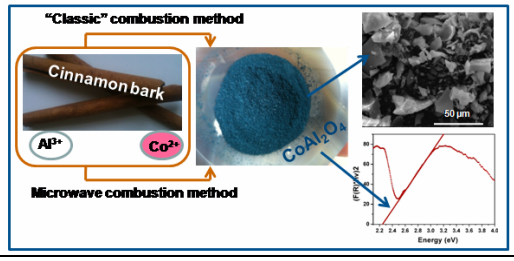

INTRODUCTION

Cobalt aluminate spinel (Thenard's blue) – $CoAl_2O_4$ – has been used since ancient times in Chinese porcelain. In 1802 it was independently discovered as a pure alumina-based spinel by Louis Jacques Thénard and for this reason, he is considered the inventor of "bright – royal blue" cobalt aluminate. Vincent van Gogh declared to his brother Theo that "Cobalt (blue) is a divine colour …there is nothing so beautiful…".

Cobalt aluminate spinel is widely used for the coloration of glass, ceramics bodies, plastics, fibers and porcelain enamels.[1,2] Due to its optical properties, it is used as color filter for automatic lamps and pigment layer on luminescent lamps in optical devices.[3] It is also used as humidity sensor,[4] ceramic catalyst in the CO_2 reforming of methane[5] and photo / electrocatalyst.[6,7]

The colour of cobalt aluminate strongly depends on its thermal stability, chemical reactivity and coordination of Co^{2+} ions in the spinel structure.[8] All these physico-chemical characteristics are crucial influenced by the synthesis method.

For this reason, in the last twenty years, the wet chemical methods have been extensively developed to synthesize $CoAl_2O_4$ nanoparticles, among them coprecipitation method,[9,10] hydrothermal/sol-gel hydrothermal and sol-gel routes[10-12] and sonochemical synthesis.[13]

Considerable efforts have been made to develop those strategies (belonging to the *chimie douce*) which are based on molecular precursors - polynuclear multimetallic compunds. These compounds provided a homogeneous distribution of the chemical species at molecular level.[14-19]

The ideal strategy of today is the combination between these methods and the green chemistry.

* Corresponding author: d_gingasu@yahoo.com

The use of plant extracts from leaves, flowers, seeds, bark or root offers the possibility of preparing nanostructured alumina – based oxides *via* several chemical pathways which are eco-friendly and clean.

The plant extracts contain a variety of polysaccharides, polyphenols, flavonoids and aminoacids which can act as reducing, stabilizing and/or chelating agents, having the possibility "to sequester" the metal ions. The interaction between these biomolecules and the metal ions at "molecular level" is the main factor in the synthesis of metal oxide nanoparticles, influencing their composition, size and shape.[20-22]

Nowadays, a variety of plant extracts such as *Aloe vera* leaves, ginger root, *Hibiscus-rosa sinensis* flowers/leaves, etc. are used to obtain metal oxide and mixed metal oxide nanoparticles.[20,22]

There are only few studies on the biosynthesis of alumina based spinel nanoparticles using plant extracts. In 2014, C. Ragupathi group published the first studies on the synthesis of MAl_2O_4 (where M(II) = Cu(II), Co(II), Ni(II), Zn(II)) using *Aloe vera* leaf extract.[23-27] In 2016, S. Moortheswaran *et al.* obtained $CoAl_2O_4$ through "one – pot combustion synthesis" using *Opuntia dilleni* extract.[28]

It is important to evaluate the possibility of using other plant extract for obtaining cobalt aluminate nanoparticles. For this reason, the cinnamon (*Cinnamon zeylanicum*) bark aqueous extract was chosen.

Cinnamon zeylanicum is a small evergreen tree belonging to the *Lauraceae* family. Due to its antibacterial, antifungal, analgesic and antioxidant activities, it is very important in human health. According to the traditional Chinese medicine cinnamon has been used as a neuroprotective agent and for the treatment of diabetes.[29]

The chemical components of cinnamom bark include essential oils, resineous compounds, cinnamic acid, cinnamaldehyde, ethyl cinnamates and eugenol.[30]

The goal of this research is to obtain cobalt aluminate ($CoAl_2O_4$) nanoparticles using cinnamon bark aqueous extract through "classic" combustion (CCM) and microwave combustion (MCM) methods.

EXPERIMENTAL

Materials

The aluminum nitrate ($Al(NO_3)_3 \cdot 9H_2O$) and cobalt nitrate ($Co(NO_3)_2 \cdot 6H_2O$) were of reagent quality (Merck). Cinnamon bark (Cinnamon / Dalchini) was from Pro Nature Organic Foods Pvt. Ltd., Bangalore, Karnataka.

Preparation of cinnamon bark extract

Cinnamon powder (2.5 g) was placed in 100 ml distilled water under stirring. The mixture was boiled for 5 min and then was filtered. The orange extract (pH = 6) was cooled at room temperature.

Synthesis of cobalt aluminate nanoparticles through "classic" combustion method (CCM)

The metal nitrates ($2Al^{3+}$:$1Co^{2+}$) were dissolved in the cinnamon aqueous extract under stirring for 3 h at room temperature. This pink solution (pH = 2) was evaporated/dried in an oven at 80 ^oC. Then the light pink compound was placed in the furnace for 2 h at 1000 ^oC. Initially, it decomposed by spontaneous self-ignition, leaving behind voluminous dark blue powder (**C12**).

The self–combustion reaction is an exothermic redox process in which the nitrates are the oxidants and the cinnamon aqueous extract plays the role of fuel (reducing agent).

Synthesis of cobalt aluminate nanoparticles through microwave combustion method (MCM)

The precursor pink solution prepared as above was placed in a domestic microwave oven (2.45 GHz, 900 W) for 15 min. The solution was boiled, underwent dehydration followed by a violent decomposition with the evolution of gases. An intense blue compound was instantly formed. In order to improve the crystallinity of the sample, the blue powder was calcined at 1000 ^oC/ 2h (**C13**).

Characterization techniques

Powder X-ray diffraction patterns were recorded using Rigaku's Ultima IV multipurpose diffraction system. The diffractometer was set in parallel beam geometry, using Cu Kα radiation (λ = 1.5406 Å), CBO optics and graphite monochromator, and operated at 40 kV and 30 mA. The measurements were performed in the θ-2θ mode, with a 0.02º step size and $5^o min^{-1}$ scan speed. Phase identification was performed using a Rigaku's PDXL software, connected to ICDD PDF-2 database. The lattice constants were refined using the Whole Powder Pattern Fitting (WPPF) and the crystallite size was calculated through the Williamson-Hall method.

The morphology of the $CoAl_2O_4$ nanoparticles was analyzed by scanning electron microscopy (FE-SEM), using a high resolution FEI QUANTA INSPECT F microscope with field emission gun (FEI Co., the Nederlands). For a high-accuracy estimation of the size and crystallinity degree of the mentioned particles, additional transmission electron microscopy (TEM / HR-TEM) and selected area electron diffraction (SAED) investigations were performed. The bright-field and high resolution images were collected by means of a Tecnai^{TM} G^2 F30 S-TWIN transmission electron microscope (FEI Co., the Nederlands), equipped with energy-dispersive X-ray analysis (EDX) for checking the elemental composition. The average particle size for both powdered samples (C12 and C13) was determined using the OriginPro 9.0 software (statistics on column) by taking into account size measurements on ~ 60 particles (from images of appropriate magnifications obtained from various microscopic fields) performed by means of the software of the electron microscopes (Digital Micrograph 1.8.0 in the case of the transmission electron microscope).

The surface analysis performed by X-Ray Photoelectron Spectroscopy (XPS) was carried out on Quantera SXM

equipment, with base pressure of 10^{-9} Torr in the analysis chamber. The X-ray source was Al K_α radiation (1486.6 eV, monochromatized) and the overall energy resolution was estimated at 0.65 eV by the full width at half maximum (FWHM) of the $Au4f_{7/2}$ line. In order to take into account the charging effect on the measured Binding Energies (BEs), the spectra were calibrated using the C1s line (BE = 284.8 eV, C-C (CH)n bondings) of the adsorbed hydrocarbon on the sample surface. A dual beam neutralizing procedure (e^- and Ar^+ ion beams) was used to compensate the charging effect in the insulating samples.

The IR spectra were recorded on KBr pellets with a JASCO FTIR 4100 spectrophotometer in the 4000–400 cm^{-1} range.

The absorption spectra were made with a JASCO V-670 spectrophotometer with solid sample accessory.

RESULTS AND DISCUSSION

Self propagating combustion process also known as solution combustion synthesis (SCS) belongs to the "chimie douce" synthesis strategies in which the precursors of the mixed oxides are "real single molecular compounds".[31]

The formation of such precursors influences the homogeneity and the stoichiometry of the cobalt aluminate spinel oxides.

To identify and to characterize the cobalt aluminate spinels XRD, SEM, TEM, XPS, FTIR and UV-Vis spectroscopy have been achieved.

The phase composition was established by X-ray diffraction patterns (Fig.1). All the peaks can be indexed to the single phase $CoAl_2O_4$ spinel (ICDD 082-2249), space group Fd-3m.

The lattice parameter *a* was 8.098±0.003 Å for **C12** and 8.097±0.003 Å for **C13**, in good agreement with the literature.[26,27] The crystallite size was 15.6 nm for **C12** and 14.9 nm for **C13**.

Low magnification FE-SEM images show, for both samples **C12** and **C13**, the presence of non-uniform aggregates with spongy aspect (Figs. 2a and 2c), which seem to be more fragmented in the case of the sample **C13** (Fig. 2c). The higher magnification FE-SEM images of Figs. 2b and 2d indicate that actually these aggregates represent compact, partially sintered blocks, consisting of equiaxial particles, with size in the nanometer range. One can notice that the particles which make up the aggregates of sample **C12** are more homogeneous as size and shape than the particles inside the aggregates of sample **C13**. However, in order to have an accurate estimation of the average particle size, TEM investigations are required.

In the case of the two powdered samples, the TEM images of Figs. 3a and 4a clearly emphasize the structuring inside the dense, partially sintered blocks, where particles are tightly bound together. It is worthy to mention that the aggregates seem to be denser and the constituent particles are more uniform as shape and size in the case of the $CoAl_2O_4$ powder prepared by the "classic" combustion method (**C12**) (Fig. 3a).

For the powder prepared by the microwave combustion method (**C13**), the TEM results support the FE-SEM observations. Thus, for this sample, unevenly sized and irregularly shaped particles, showing a tendency to a duplex-type morphology, were observed. In this case, a major fraction of rather spherical, small (< 15 nm) nanoparticles coexists with a minor amount of larger (50-60 nm), well faceted, polyhedral, but thinner particles, with well defined edges and corners.

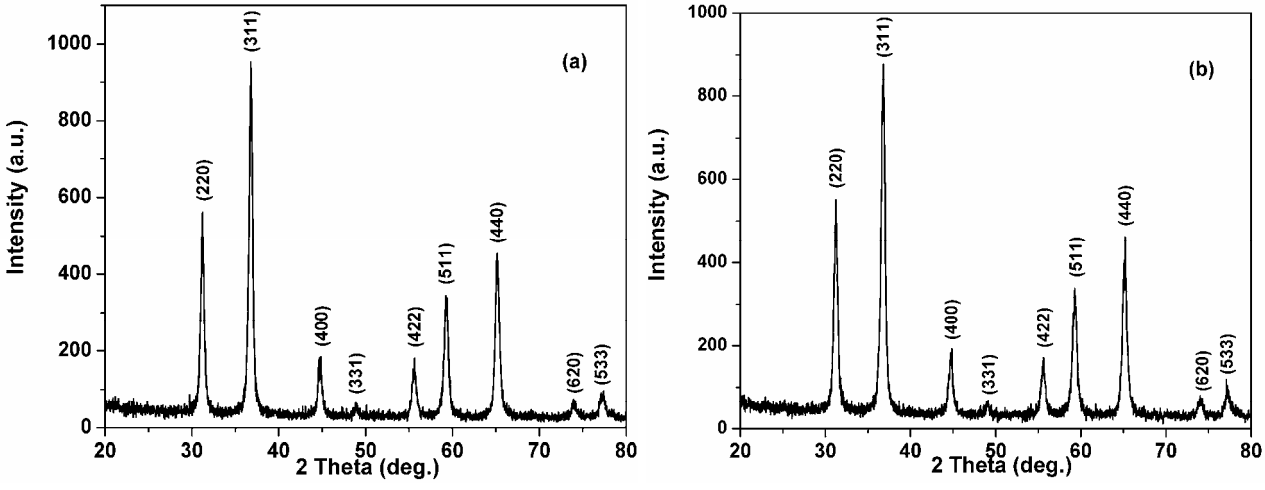

Fig. 1 – X-ray diffraction of the cobalt aluminates: (a) **C12**, (b) **C13**.

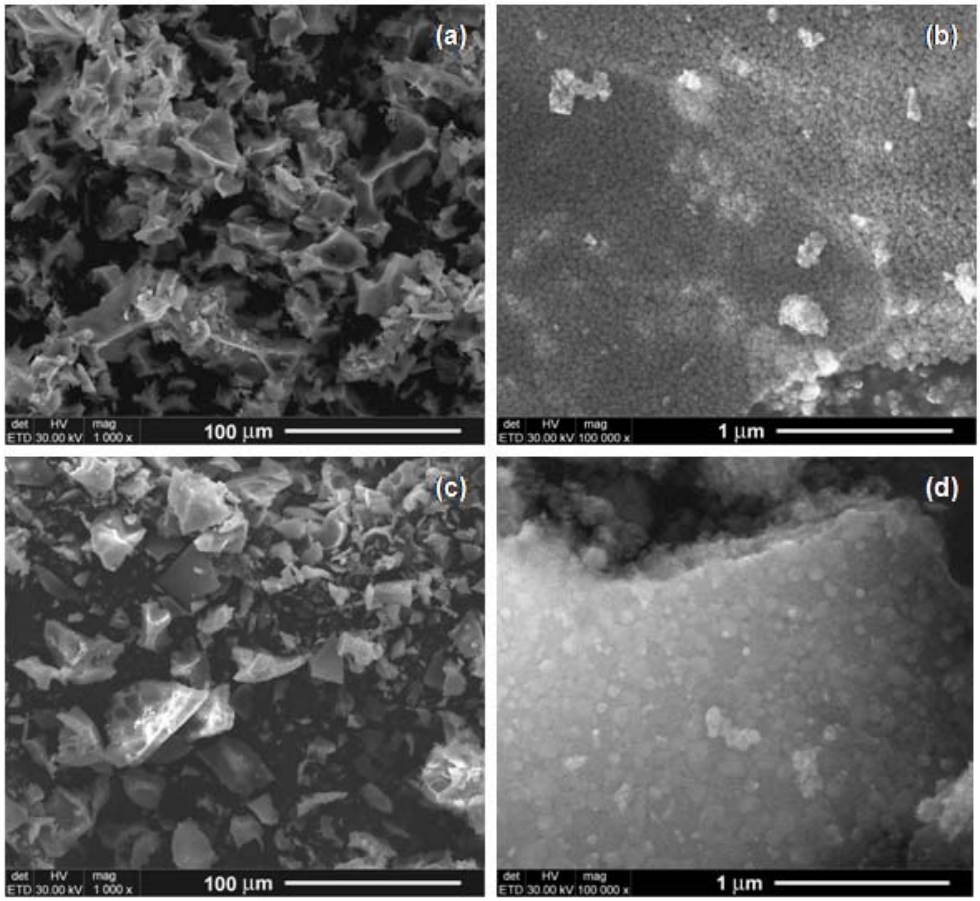

Fig. 2 – SEM images of samples **C12** [(a), (b)] and **C13** [(c), (d)]: (a) and (c) - general views; (b) and (d) - details.

For both powdered samples, size measurements on ~ 60 particles performed on images obtained from various microscopic fields, indicated unimodal particle size distributions (Figs. 3b and 4b), but a broader one in the case of sample **C13**, due to the above-mentioned particular morphology (Fig. 4b). Average particle sizes of (20.5 ± 5.2) nm and of (19.1 ± 5.9) nm were determined for the samples **C12** and **C13**, respectively. These values are roughly in agreement (they are found in the margin of error of measurement) with the values of the mean crystallite sizes calculated based on XRD data, demonstrating the single crystal nature of the particles of both powders.

The HRTEM images of Figs. 3c and 4c show long-range highly ordered fringes of some adjacent particles, with spacing at 2.33 and 2.86 Å, respectively, corresponding to the (2 2 0) and (2 2 2) crystalline planes of the cubic spinel structure (space group Fd-3m) of $CoAl_2O_4$ (ICDD no. 00-038-0814). The high crystallinity degree of the randomly oriented particles in the aggregates of both $CoAl_2O_4$ powders is also pointed out by the bright spots, forming well-defined, concentric diffraction rings, assigned to several crystalline planes of the unique spinel phase in the SAED patterns of the **C12** and **C13** samples (Figs. 3d and 4d). The uniformity degree of the particle sizes is also emphasized by the aspect of the spots in the diffraction rings. Thus, while for the evenly sized particles of sample **C12** the brightness and size of the spots is almost similar, contributing to a "continuous" aspect of the diffraction rings, in the case of the non-uniform particles of sample **C13**, larger and brighter spots coexist with smaller and less visible ones, giving a "dashed" aspect of the corresponding diffraction rings.

X-ray photoelectron spectroscopy analysis was performed in order to highlight the chemical elements and their oxidation states detected on the outermost surface layer (~ 10 nm). The XPS spectra recorded on the two samples are very similar. For this reason, in Fig. 5 are presented, as example, the XPS spectra recorded for cobalt aluminate obtained through classic combustion (**C12**). Thus, survey spectrum revealed the presence of C, O, Co and Al on the surface. The high resolution spectra for the most prominent transitions Co2p, Al2p and O1s were recorded.

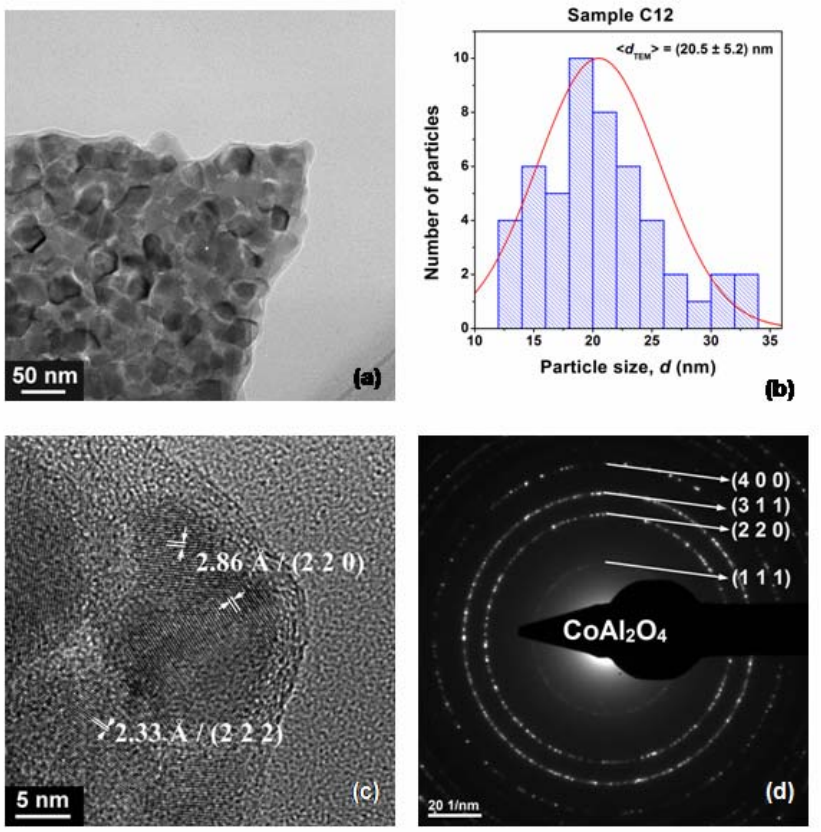

Fig. 3 – (a) TEM image, (b) particle size distribution histogram, (c) HRTEM image and (d) SAED pattern of sample **C12**.

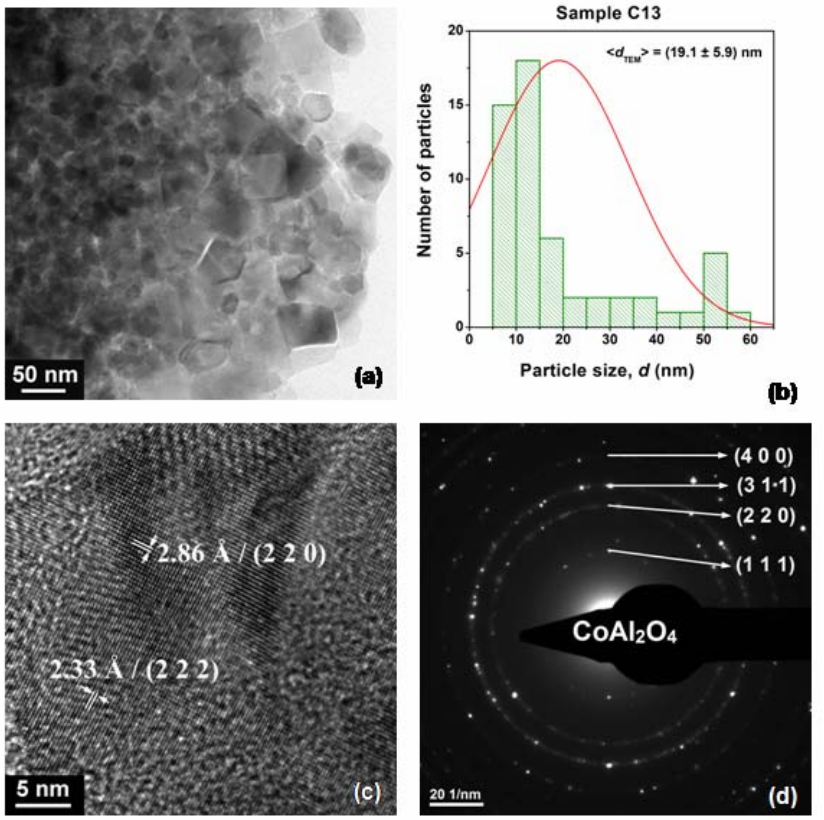

Fig. 4 – (a) TEM image, (b) histogram indicating the particle size distribution obtained from measurements performed on several TEM images, (c) HRTEM image and (d) SAED pattern and of sample **C13**.

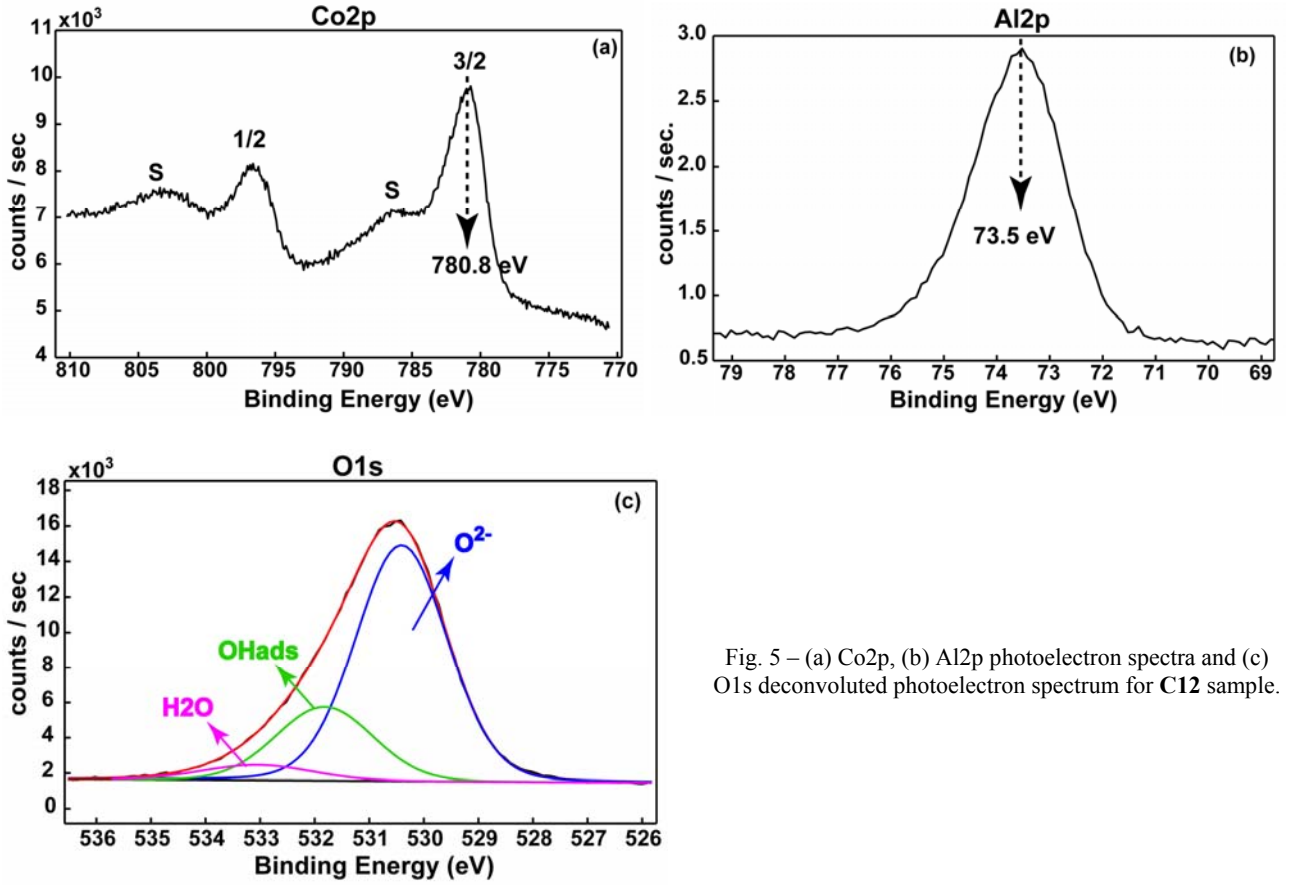

Fig. 5 – (a) Co2p, (b) Al2p photoelectron spectra and (c) O1s deconvoluted photoelectron spectrum for **C12** sample.

The binding energies (BEs) for the doublet Co2p3/2 and Co2p1/2 were determined experimentally as 780.8 eV and 795.8 eV (Fig. 5a), respectively. These values are characteristic to Co^{2+} ions tetrahedrally coordinated into $CoAl_2O_4$ spinel structure, according to XRD pattern. It is worth to mention that the associated satellites observed at ~ 786 eV and ~ 803 eV also proved the presence of Co^{2+}.

As shown in Fig. 5b, Al2p binding energy at 735 eV indicates the presence of Al^{3+} octahedrally coordinated (corroborated with FTIR and XRD results). Following the quantification procedure, the experimental stoichiometry close to the ratios Co:Al:O = 1:2:4 within the experimental errors (±5%) was found.

The O1s spectrum was fitted into three peaks at 530.2, 531.7, 533.0 which were assigned as follow: oxygen bond in the spinel lattice, OH adsorbed on the surface as well as a small amount of adsorbed H_2O (Fig. 5c).

In order to sustain the formation of the cobalt aluminate spinel phase, the FTIR spectra of the samples **C12** and **C13** were recorded between 4000 cm^{-1} and 400 cm^{-1} (Fig. 6). Three very strong bands are observed around 670 cm^{-1}, 550 cm^{-1} and 500 cm^{-1} assigned to the vibrations of M-O, Al-O and M-O-Al bending vibrations of AlO_6 octahedra groups in the $CoAl_2O_4$ pure phase. According to Tarte,[32] the strong band observed in the range 650 - 680 cm^{-1} (at ~ 670 cm^{-1} for **C12** and at ~ 663 cm^{-1} for **C13**) is an Al-O stretching vibration of the AlO_6 lattice - "condensed AlO_6".

Both spectra presented very weak bands at ~ 3400 cm^{-1} and ~1600 cm^{-1} which can be assigned to the vibrations of water molecules adsorbed on the surface of crystallites.[26,27]

The absorbance spectra recorded for both samples in the range 200 nm – 1800 nm are shown in Fig. 7. These spectra present very intense bands at 600 - 800 nm and 1200 - 1700 nm characteristic to the Co^{2+} ions in the tetrahedral configuration. They are associated to $^4A_2(F) \rightarrow {}^4T_1(P)$ (ν_3) and $^4A_2(F) \rightarrow {}^4T_1(F)$ (ν_2) transitions, respectively. The fine splitting of the first band is due to the spin orbit coupling between the excited and the neighboring doublet states $^2A_1(G)$ and $^2T_{2g}(G)$. Because of the mixing of quartet and doublet states, the spin selection rule is relaxed and the transition is allowed.[33]

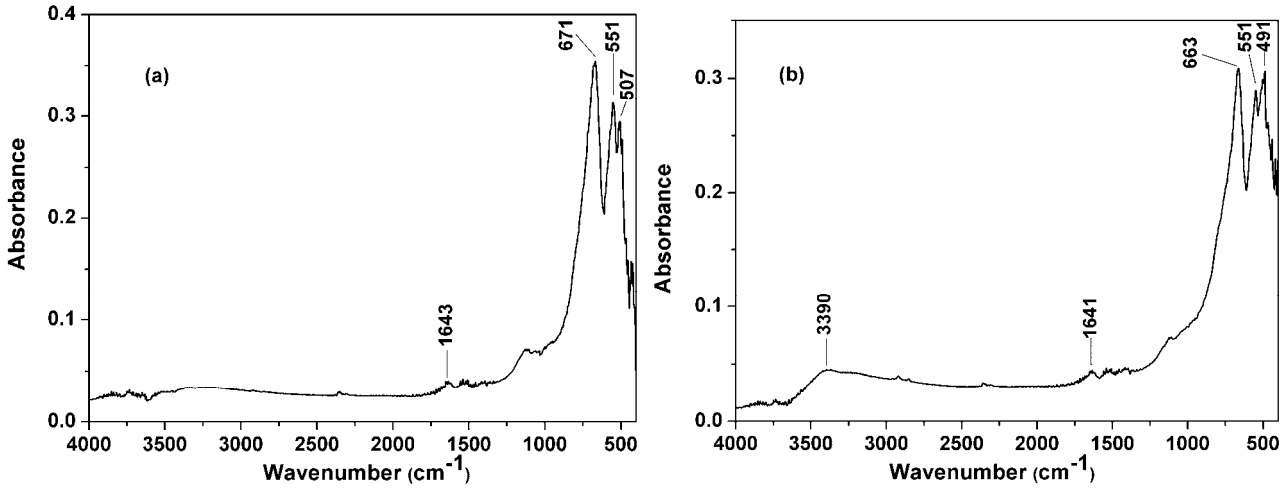

Fig. 6 – IR spectra of the $CoAl_2O_4$ spinel: (a) **C12**, (b) **C13**.

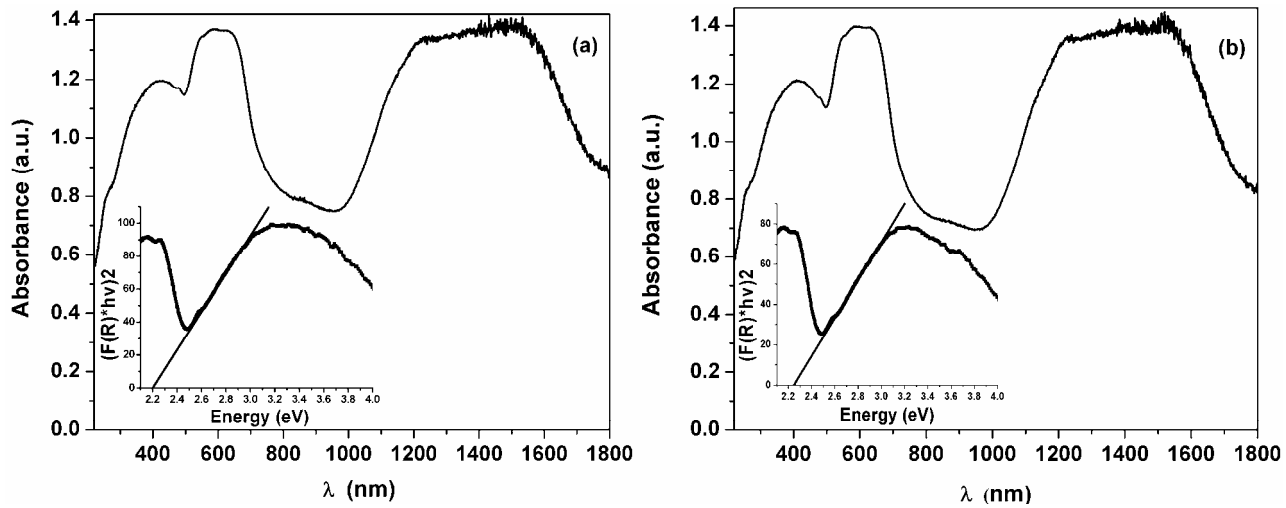

Fig. 7 – Absorption spectra and band gap (inset) of the $CoAl_2O_4$ spinel: (a) **C12**, (b) **C13**.

The optical properties of cobalt aluminate spinels (**C12** and **C13**) show an energy band gap in the range 2.20 – 2.25 eV (Fig. 7 inset). These calculated band gap values indicate that $CoAl_2O_4$ spinel oxide is intrinsically p-type conductivity.[34]

CONCLUSIONS

Cobalt aluminate spinel nanoparticles were successfully obtained through "classic" and microwave combustion methods using cinnamon bark aqueous extract. The XRD patterns indicated the crystallization of the cubic spinel structure; no other phases were identified in the samples. SEM images revealed that the particles of the sample obtained through "classic" combustion (**C12**) are more homogeneous as size and shape than those obtained through microwave combustion (**C13**). The TEM images sustain this conclusion. For both samples, the size measurements indicated unimodal particle size distributions, broader one in the case of the sample **C13**. The average sizes are roughly in agreement with those obtained from XRD data. The XPS spectra have been highlighted the presence of Co^{2+} ions tetrahedrally coordinated into the $CoAl_2O_4$ spinel structure. The formation of the cobalt aluminate spinel is also supported by the FTIR spectra. The band gap energies in the range 2.20-2.25 eV confirmed the p-type behavior of $CoAl_2O_4$ spinel oxides.

Acknowledgments: Support of the EU (ERDF) and Romanian Government under POS-CCE O 2.2.1 project INFRANANOCHEM - Nr. 19/01.03.2009, allowing the acquisition of the research infrastructure, is gratefully acknowledged. The work also benefits from the support of the "Materials Science and Advanced Characterization Methods" Programme of the "Ilie Murgulescu" Institute of Physical Chemistry, financed by the Roumanian Academy.

REFERENCES

1. L. K. C. de Souza, J. R. Zamian, G. N. da Rocha Filho, L. E. B. Soledade, I. M. G. dos Santos, A. G. Souza, T. Scheller, R. S. Angélica and C. E. F. da Costa, *Dyes Pygments*, **2009**, *81*, 187-192.
2. I. Mindru, D. Gingasu, G. Marinescu and L. Patron, "Design de nanomateriale oxidice cu structură spinelică. De la sinteză la aplicații" (Design of Spinelic Oxides Nanomaterials. From Synthesis to Applications), Matrix Rom, Bucureşti, 2008.
3. D. M. A. Melo, J. D. Cunha, J. D. G. Fernandes, M. I. Bernardi, M. A. F. Melo and A. E. Martinelli, *Mater. Res. Bull*., **2003**, *38*, 1559-1564.
4. J. J. Vijaya, L. J. Kennedy, G. Sekaran, B. Jeyaraj and K. S. Nagaraja, Sens. *Actuat. B-Chem*., **2007**, *123*, 211-217.
5. L. Ji, S. Tang, H. C. Zeng, J. Lin and K. L Tan, *Appl. Catal. A-Gen.*, **2001**, *207*, 247-255.
6. S. Rahnamaeiyan, M. Nasiri, R. Talebi and S. Khademolhoseini, *J. Mater. Sci.-Mater. El.*, **2015**, *26*, 8720-8725.
7. R. Dumitru, F. Manea, L. Lupa, C. Păcurariu, A. Ianculescu, A. Baciu and S. Negrea, *J. Therm. Anal. Calorim.*, **2017**, 128, 1305-1312.
8. W. Li, J. Li and J. Guo, *J. Eur. Ceram. Soc.*, **2003**, *23*, 2289-2295.
9. S. Britto, A. V. Radha, N. Ravishankar and P. V. Kamath, *Solid State Sci.*, **2007**, *9*, 279-286.
10. M. Peymannia, A. Soleimani-Gorgani, M. Ghahari and M. Jalili, *Ceram. Int.*, **2015**, *41*, 9115-9121.
11. J. Lu, K. Minami, S. Takami and T. Adschiri, *Chem. Eng. Sci.*, **2013**, *85*, 50-54.
12. F. Yu, J. Yang, J. Ma, J. Du and Y. Zhou, *J. Alloys Compd.*, **2009**, *458*, 27-32.
13. W. Lv, Q. Qiu, F. Wang, S. Wei, B. Liu and Z. Luo, *Ultrason. Sonochem*., **2010**, *17*, 793-801.
14. S. I. Ahmed, *Mater. Res. Bull*., **2011**, *46*, 2548-2553.
15. P. S. Salem, *Ceram. Int.*, **2016**, *42*, 2548-2553.
16. I. Mindru, G. Marinescu, D. Gingasu, L. Patron, C. Ghica and M. Giurginca, *Mater. Chem. Phys.*, **2010**, *122*, 491-497.
17. S. Ummartyotin, S. Sangngern, A. Kaewvilai, N. Koonsaeng, H. Manuspiya and A. Laobuthee, *J. Sustainable Energy and Environ.*, **2009**, *1*, 31-37.
18. L. Gama, M. A. Ribeiro, B. S. Barros, R. H. A. Kiminami, I. T. Weber and A. C. F. M. Costa, *J. Alloys Compd.*, **2009**, *483*, 453-455.
19. M. Gaudon, L. C. Robertson, E. Lataste, M. Duttine, M. Ménétrier and A. Demourgues, *Ceram. Int.,* **2014**, *40*, 5201-5207.
20. O. V. Kharissova, H. V. Rasika Dias, B. I. Kharisov, B. O. Pérez and V. M. J. Pérez, *Trends Biotechnol.*, **2013**, *31*, 240-248.
21. M. Rai and A. Yadav, *JET Nanotechnology*, **2013**, *7*, 117-124.
22. R. S. Varma, *Curr. Opin. Chem. Eng.*, **2012**, *1*, 123-128.
23. C. Ragupathi, J. J. Vijaya, P. Surendhar and L. J. Kennedy, *Polyhedron*, **2014**, *72*, 1-7.
24. C. Ragupathi, L. J. Kennedy and J. J. Vijaya, *Adv. Powder Technol*., **2014**, *25*, 267-273.
25. C. Ragupathi, J. Judith Vijaya, L. John Kennedy and M. Bououdina, *Mater. Sci. Semicond. Process.*, **2014**, *24*, 146-156.
26. C. Ragupathi, J. J. Vijaya, L. J. Kennedy and M. Bououdina, *Ceram. Int.*, **2014**, *40*, 13067-13074.
27. C. Ragupathi, J. J. Vijaya, S. Narayanan, S. K. Jesudoss and L. J. Kennedy, *Ceram. Int.*, **2015**, *41*, 2069-2080.
28. S. Moortheswaran, A. Manikandan, S. Sujatha, S.K. Jaganathan and S.A. Antony, *Nanosci. Nanotech. Lett.*, **2016**, *8*, 424-427.
29. S. F. Nabavi, A. Di Lorenzo, M. Izadi, E. Sobarzo-Sánchez, M. Daglia and S. M. Nabavi, *Nutrients*, **2015**, *7*, 7729-7748.
30. B. Adinew, *Int. J. Herb. Med.*, **2014**, *1*, 22-31.
31. A. Sharma, O. P. Modi and G. K. Gupta, *Adv. Appl. Sci. Res.*, **2007**, *459*, 214-222.
32. P. Tarte, *Spectrochim. Acta*, **1967**, *23 A*, 2127-2143.
33. A. B. P. Lever, "Inorganic electron spectroscopy", Elsevier, Wiley, New York, 1986.
34. A. Walsh, Y. Yan, M. M. Al-Jassim and S.-H. Wei, *J. Phys. Chem. C*, **2008**, *112*, 12044-12050.